

gives

$$t_{CR} = k \log_e \left[1 + \frac{4}{a_0^2} \right] \quad (6.14)$$

In consideration of the solutions for $m=1$ and $m=3$, we may note the following points about the creep buckling process:

1. Whereas elastic or elasto-plastic buckling corresponds to the existence of many equilibrium configurations corresponding to loads beyond the critical, creep buckling is characterized by deflections or velocities that increase beyond all bounds.
2. Creep buckling can occur at a finite time only for a nonlinear creep law.
3. Creep buckling will occur at any axial compressive load no matter how small. The pertinent question becomes: Is t_{CR} less than or greater than the intended design life?
4. Creep buckling will occur only if the column has initial imperfections. Otherwise an infinite time for creep buckling is obtained from Eq. (6.14) with $a_0=0$. In practical structures there is always an initial imperfection.
5. The critical time depends strongly on the axial load but not so strongly on the initial shape.
6. Small deflection theory is not really valid near t_{CR} as the deflections are growing rapidly. We have made the assumption in order to present the behavior.
7. The Euler load for the instantaneous buckling does not appear in the above solution because the initial elastic strains were not included in the analysis. The Euler load is the instantaneous critical load of an elastic column.

6.2.2 Tangent Modulus Approach

The column buckling problem may also be solved empirically by the tangent modulus approach of Shanley [7]. In a consideration of columns that were loaded beyond the yield prior to buckling he reasoned as follows: since there are always slight imperfections in construction the progress of deflection of the column is such that both sides, the concave and the convex, are always in a state of compression. The process of loading for several increments is shown in Fig. 6.1. During strain increments 1 to 5 in the illustration, the straining is essentially uniform.

(6.14)

we may note the
 depends to the ex-
 sponding to loads
 by deflections or
 a nonlinear creep
 e load no matter
 t_{CR} less than or
 initial imperfec-
 is obtained from
 re is always an
 oad but not so
 s the deflections
 on in order to
 s not appear in
 s were not in-
 taneous critical

rically by the
 on of columns
 s reasoned as
 nstruction the
 s, the concave
 he process of
 s strain incre-
 ally uniform.

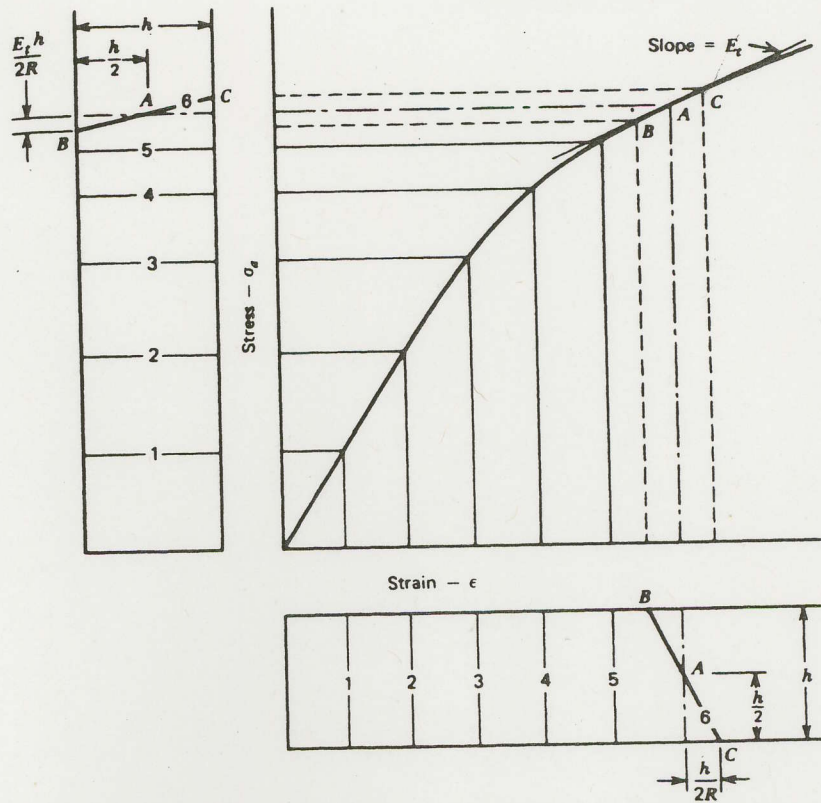


Fig. 6.1 Strain and stress distributions for an inelastic column with small initial imperfections—tangent modulus model. Courtesy of McGraw-Hill Book Co., Inc., G. Gerard, Introduction to Stability Theory (1962).

Increment 6 is approaching the critical strain, and axial straining and bending occur simultaneously. Since there is no reversal of strain on the convex side, all points lie along the path BAC on the stress-strain curve. By representing the curve locally at A by the tangent modulus the stress distribution becomes a linear function of the strain, and the critical load of the column can be obtained in the usual way, as follows, for a simply supported column with an initial shape w_0 . In this case the moment equilibrium equation becomes

$$\frac{d^2 w}{dx^2} + \frac{P_0}{E_t I} (w_0 + w) = 0 \tag{6.15}$$

Here w is the part of the deflection that is caused by bending, E_t is the

tangent modulus, and I is the moment of inertia of the column cross-section. Now assume that the initial shape is given by the Fourier series

$$w_0 = \sum_{n=1}^{\infty} \bar{w}_n \sin \frac{n\pi x}{L} \quad (6.16)$$

and assume that the deflection solution is given by the Fourier series

$$w = \sum_{n=1}^{\infty} w_n \sin \frac{n\pi x}{L} \quad (6.17)$$

which satisfies the end condition of simple support. If Eqs. (6.16) and (6.17) are substituted into Eq. (6.15), we obtain

$$\sum_{n=1}^{\infty} \left[-w_n + \frac{P_0 L^2}{n^2 \pi^2 E_t I} (\bar{w}_n + w_n) \right] \sin \frac{n\pi x}{L} = 0 \quad (6.18)$$

To obtain a nontrivial solution of this for arbitrary values of x we set the square bracket to zero and find

$$w_n = \frac{\bar{w}_n}{\frac{n^2 \pi^2 E_t I}{L^2 P_0} - 1} \quad (6.19)$$

This solution becomes unbounded when the denominator goes to zero, at a load

$$P_{0_{CR}} = \frac{n^2 \pi^2 E_t I}{L^2} \quad (6.20)$$

The lowest value of this pertains to $n=1$

$$P_{0_{CR}} = \frac{\pi^2 E_t I}{L^2} \quad (6.20a)$$

For the elastic case $E_t = E$ and the result is called the Euler load. We have, however, considered the case where P_0/A exceeds the yield, according to Shanley's tangent modulus approach.

To apply this approach to creep we require E_t as a function of time. We have introduced a means of providing this via the isochronous stress-strain curves in Fig. 1.10. To use these in predicting creep buckling we first

rearrange Eq. (6.20a)

$$E_{tCR} = \frac{P_0 L^2}{I \pi^2} = \frac{\sigma L^2 A}{I \pi^2} \tag{6.20b}$$

where $\sigma = P_0/A$ and E_{tCR} is the critical tangent modulus. We now say that the column buckles at σ when E_t becomes E_{tCR} . The value of E_{tCR} is obtained from the load on the column and its geometry by Eq. (6.20b). We now notice from the isochronous stress-strain curves of Fig. 1.10 that at a given stress E_t decreases with time. Thus we read horizontally at the stress σ of the column and load and at some time we reach a curve with slope E_{tCR} . This time becomes the critical time for buckling. The approach, which is graphical, can be somewhat simplified if we accept the power law in steady creep, that is

$$\dot{\epsilon} = \left(\frac{\sigma}{\sigma_c} \right)^m \tag{6.21}$$

Then the strain is, on integration

$$\epsilon - \epsilon_0 = \left(\frac{\sigma}{\sigma_c} \right)^m t \tag{6.22}$$

where ϵ_0 is the initial strain at $t=0$. The tangent modulus theory uses

$$E_t = \frac{d\sigma}{d\epsilon} \tag{6.23}$$

Thus if we differentiate Eq. (6.22) we get, for constant t ,

$$d\epsilon = \frac{m}{\sigma_c} \left(\frac{\sigma}{\sigma_c} \right)^{m-1} t d\sigma \tag{6.24a}$$

from which

$$E_t = \frac{d\sigma}{d\epsilon} = \frac{1}{\frac{m}{\sigma_c} \left(\frac{\sigma}{\sigma_c} \right)^{m-1} t} \tag{6.24b}$$

Now Eqs. (6.20b) and (6.24b) give

$$t_{CR} = \frac{I \pi^2}{\sigma L^2 A} \frac{1}{\frac{m}{\sigma_c} \left(\frac{\sigma}{\sigma_c} \right)^{m-1}} \tag{6.25}$$

a of the column cross-
by the Fourier series

(6.16)

the Fourier series

(6.17)

ort. If Eqs. (6.16) and

$$\frac{\pi x}{L} = 0 \tag{6.18}$$

values of x we set the

(6.19)

ator goes to zero, at a

(6.20)

(6.20a)

Euler load. We have,
ie yield, according to

function of time. We
chronous stress-strain
ep buckling we first

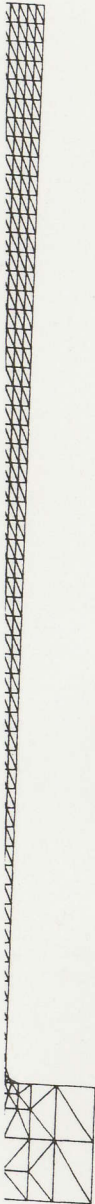


Fig. 8.14 Geometry and finite element breakup for circular plate test [14]. Courtesy of the Oak Ridge National Laboratory.

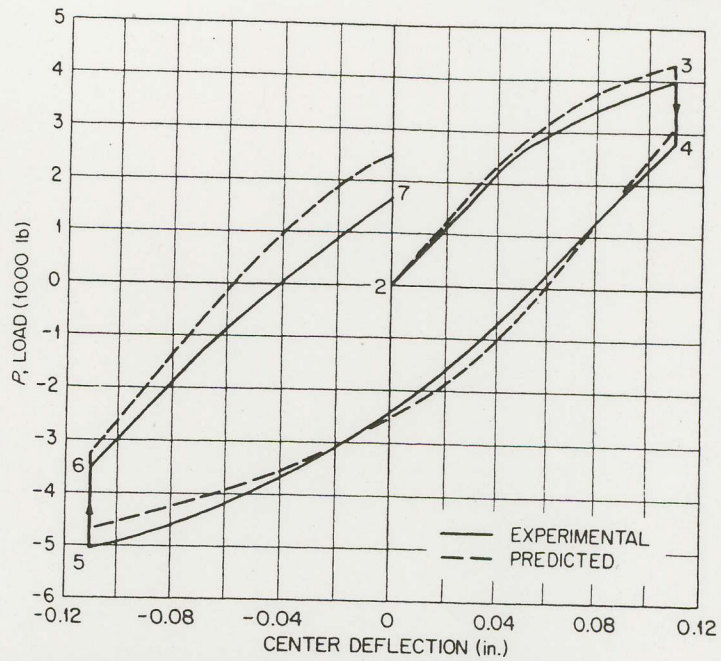


Fig. 8.15 Comparison of measured and predicted load-deflection response of circular plate. Numbered points correspond to points in the load history of Fig. 8.13 [14]. Courtesy of the Oak Ridge National Laboratory.

value of the center deflection was 0.11 in. The hold time periods shown in Fig. 8.14 were each nominally 144 hours and the plate deflection went from zero to maximum and back down in 30 sec. each.

The plate test was analyzed by Clinard et al. [14] using the finite element program, PLACRE [15]. The specimen and its finite element breakup are shown in Fig. 8.14. The model consisted of 784 three-node axisymmetric, triangular ring elements. Fig. 8.15 compares the calculated and the measured loads that were required to produce the short time central deflection changes. Fig. 8.16 compares the calculated and predicted load response during the two hold periods in the cycle. The agreement between the calculated and measured results is good. Fig. 8.16, in particular, demonstrates the adequacy of using the creep law for relaxation analysis, as discussed in Chapter 2.

8.4.6 Creep Buckling of an Axially Compressed Cylindrical Shell

In Chapter 6 we applied the methods that were described to the creep buckling tests of axially loaded shells carried out by Samuelson [21]. One

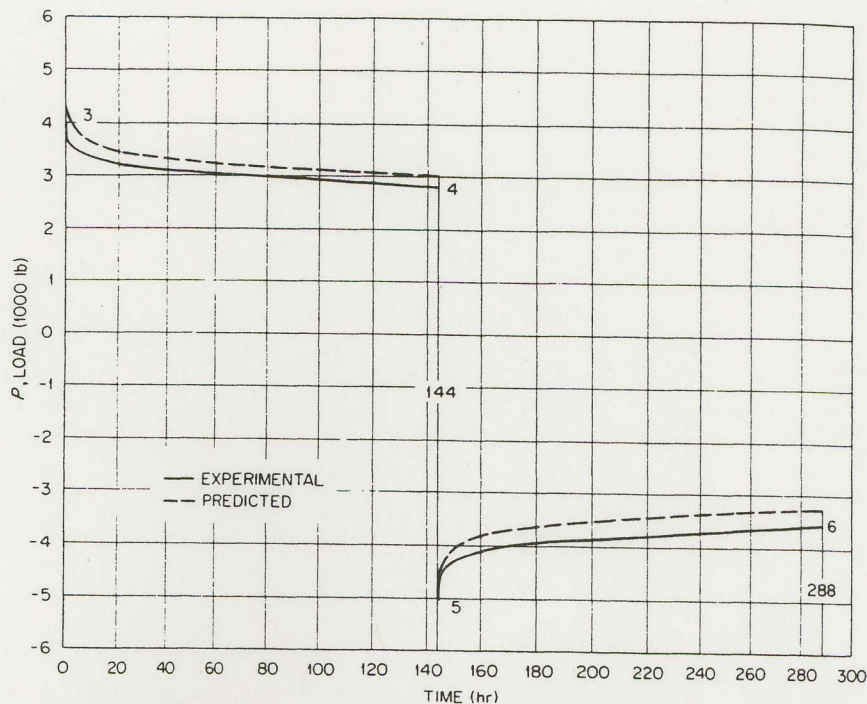


Fig. 8.16 Comparison of measured and predicted load-time response for circular plate. Numbered points correspond to points in the load history of Fig. 8.13 [14]. Courtesy of the Oak Ridge National Laboratory.

of these tests was analyzed by Stone and Nickell [22] with the finite element program, MARC, to which we referred in Section 8.3.2. In particular, they considered the case with radius to thickness ratio of 32 and applied axial stress equal to 12.1 kg/mm^2 , which is included in Table 6.1 of Chapter 6. We may recall that the buckling time measured was 7.2 hours and there were several predictions based on the methods of Chapter 6 given as 11.5, 10.5, 9.12, and 8.30 hours.

In the finite element runs the creep was assumed to be stationary with a steady creep law

$$\dot{\epsilon}^C = 4.4(10^{-10})\sigma_e^{5.8}$$

Two methods were used as follows, the details of which are beyond the scope of the text. The first is a step by step method:

1. Apply the external load to the shell and solve the time independent elasto-static problem.

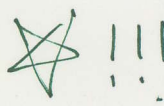
2. Begin to march in time for creep analysis, as described earlier in this chapter.
3. Stop the creep analysis at some time, t .
4. Allow a small additional time increment for creep, Δt .
5. Solve the resulting eigenvalue problem for the eigenvalue λ of the load and the eigenfunction ϕ .
6. Calculate the critical time from the formula

$$t_{CR} = t + \lambda \Delta t$$

Stone and Nickell [22] applied this approach to a model that was made up of twenty elements along the length of the shell and three elements in the thickness direction. The assembly was analyzed for one hour of creep and the critical time was found to be 69.5 hours compared to the measured value of 7.2 hours. Next, the model was changed to 50 axial shell elements and again allowed to creep for one hour. The critical time was now reduced to 19.7 hours. This is still above the experimental value of 7.2 hours and all of the approximate values from Table 6.1.

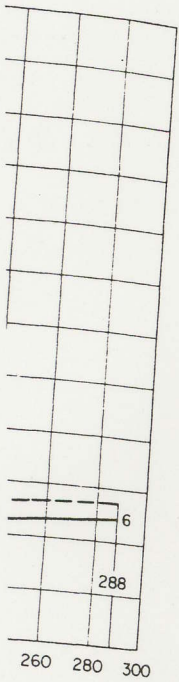
Next, it was postulated that plasticity was occurring in the regions near the shell supports. The resulting behavior was analyzed by marching in time until the structural stiffness became non-positive definite. This gave a result of 9.56 hours, at which time a plastic hinge formed at one of the edges. The remaining differences, compared to the measured value of 7.2, were attributed to the presence of imperfections in the shell and inaccuracies in ignoring the transient creep behavior. Now, however, the finite element result is within the range of the approximate results obtained by the methods of Chapter 6.

It appears, therefore, that the approximate methods are to be preferred because of their relative simplicity and accuracy. As pointed out by Stone and Nickell [22], and by Dhalla and Gallagher [9], large deflection creep buckling analyses are currently still hazardous. Work is continuing in this area.



8.4.7 Creep of a Rotating Gas Turbine Seal Ring

In gas turbine construction there is a seal ring located in the vicinity of the point of attachment between the blades and the disc. The purpose of the seal ring is to contain cooling air while keeping out the hot gases that impinge on this general area. The assembly is shown in Fig. 8.17. As shown, the ring sits on a shoulder against which it is driven by the centrifugal force produced by rotation at 12,000 rpm. The highest temperature occurs at the outer tip of the ring. It is desired to maintain the shape of the ring so as to preserve the seal during operation of the turbine.



circular plate.
Courtesy of the

the finite
8.3.2. In
of 32 and
Table 6.1
d was 7.2
of Chapter

try with a

yond the

pendent